

This article was downloaded by:

On: 23 January 2011

Access details: *Access Details: Free Access*

Publisher *Taylor & Francis*

Informa Ltd Registered in England and Wales Registered Number: 1072954 Registered office: Mortimer House, 37-41 Mortimer Street, London W1T 3JH, UK



Journal of Coordination Chemistry

Publication details, including instructions for authors and subscription information:

<http://www.informaworld.com/smpp/title~content=t713455674>

Syntheses, crystal structures, magnetic properties and theoretical analysis of two new molecular solids based on $\text{Ni}(\text{mnt})_2$

Chun-Lin Ni^a; Qian Huang^a; Hong-Rong Zuo^a; Yong Hou^a; Qing-Jin Mang^b

^a Department of Applied Chemistry, College of Science, Centre of Inorganic Functional Materials, South China Agricultural University, Guangzhou, PRC ^b State Key Laboratory of Coordination Chemistry, Coordination Chemistry Institute, Nanjing University, Nanjing, PRC

To cite this Article Ni, Chun-Lin, Huang, Qian, Zuo, Hong-Rong, Hou, Yong and Mang, Qing-Jin (2009) 'Syntheses, crystal structures, magnetic properties and theoretical analysis of two new molecular solids based on $\text{Ni}(\text{mnt})_2$ ', *Journal of Coordination Chemistry*, 62: 9, 1502 – 1512

To link to this Article: DOI: 10.1080/00958970802617585

URL: <http://dx.doi.org/10.1080/00958970802617585>

PLEASE SCROLL DOWN FOR ARTICLE

Full terms and conditions of use: <http://www.informaworld.com/terms-and-conditions-of-access.pdf>

This article may be used for research, teaching and private study purposes. Any substantial or systematic reproduction, re-distribution, re-selling, loan or sub-licensing, systematic supply or distribution in any form to anyone is expressly forbidden.

The publisher does not give any warranty express or implied or make any representation that the contents will be complete or accurate or up to date. The accuracy of any instructions, formulae and drug doses should be independently verified with primary sources. The publisher shall not be liable for any loss, actions, claims, proceedings, demand or costs or damages whatsoever or howsoever caused arising directly or indirectly in connection with or arising out of the use of this material.

Syntheses, crystal structures, magnetic properties and theoretical analysis of two new molecular solids based on $\text{Ni}(\text{mnt})_2^-$

CHUN-LIN NI*[†], QIAN HUANG[†], HONG-RONG ZUO[†],
YONG HOU[†] and QING-JIN MANG[‡]

[†]Department of Applied Chemistry, College of Science, Centre of Inorganic Functional
Materials, South China Agricultural University, Guangzhou, PRC

[‡]State Key Laboratory of Coordination Chemistry, Coordination Chemistry Institute,
Nanjing University, Nanjing, PRC

(Received 23 February 2008; in final form 1 August 2008)

Two new molecular solids, [1-(2'-Cl-4'-Rbenzyl)pyridinium][bis(maleonitriledithiolato)nickel] [abbreviated as ([ClRbzPy][Ni(mnt)₂]), R = Br(**1**), I(**2**)], have been prepared and characterized. The Ni(III) ions form a 1-D zigzag alternating chain within a Ni(mnt)₂⁻ column through Ni...S, S...S, or π...π stacking interactions in **1** and a tetramer in **2**. The variable temperature magnetic susceptibilities of **1** and **2** in the temperature range 1.8–300 K have been interpreted in terms of a simple dimer model approximation ($H = -2JS_A S_B$), revealing strong antiferromagnetic interactions with the fitting value $g = 1.98$ and $J = -231.5 \text{ cm}^{-1}$ for **1**, $g = 1.96$ and $J = -245.3 \text{ cm}^{-1}$ for **2**.

Keywords: Bis(maleonitriledithiolate)nickelate(III); Molecular solids; Pyridinium derivatives; Crystal structure; Antiferromagnetic interactions

1. Introduction

Structural and magnetic properties of molecular solids based on *bis*-dithiolate transition metal compounds is an important field of coordination chemistry, materials chemistry, and condensed matter physics [1–8]. Recent work dedicated to molecular-based magnets containing Ni(mnt)₂⁻ (mnt²⁻ = maleonitriledithiolate) is driven in part by the discovery of NH₄·Ni(mnt)₂·H₂O, which shows ferromagnetic ordering at low temperature [9]. The organic countercation of Ni(mnt)₂⁻ controls the stacking pattern of the anions with the majority of molecular solids displaying magnetic properties such as magnetic transition from ferromagnetic coupling to diamagnetism, ferromagnetic ordering, spin-gap transition, meta-magnetism, and spin-Peierls-like transitions [10–18]. Studies concerning magneto-structural correlation including theoretical calculations have indicated that the prominent structural feature is that Ni(mnt)₂⁻ and the cations stack into well-segregated columns in the solid state, and the topology and size of the

*Corresponding author. Email: scauchemnicl@163.com

countercation plays an important role in controlling the stacking and overlap of anions [19–24]. These findings prompt us to further investigate the influence of countercation on the stacking pattern and magnetic properties of molecular solids based on Ni(mnt)₂⁻ anion. The present work reports crystal structures and magnetic behavior of two newly prepared molecular solids based on Ni(mnt)₂⁻: [BrClBzPy][Ni(mnt)₂] (**1**) and [IClBzPy][Ni(mnt)₂] (**2**) ([BrClBzPy]⁺ = 1-(2'-chloro-4'-bromobenzyl)pyridinium and [IClBzPy]⁺ = 1-(2'-chloro-4'-iodobenzyl)pyridinium).

2. Experimental

2.1. General materials and physical measurements

All reagents used in the syntheses were of analytical grade. [BrClBzPy]Br and [IClBzPy]Br were prepared by the literature method [25]. Disodium maleonitridedithiolate (Na₂mnt) was synthesized by a published procedure [26], and a similar method for preparing [BrFBzPy]₂[Ni(mnt)₂] was used to prepare [BrClBzPy]₂[Ni(mnt)₂] and [IClBzPy]₂[Ni(mnt)₂] [15]. Elemental analyses for C, H, and N were determined on a Model 240 Perkin Elmer CHN analytical instrument. IR spectra with KBr pellets were obtained with a VECTORTM 22 FT-IR (400–4000 cm⁻¹) spectrophotometer. Electrospray mass spectra [ESI-MS] were determined on a Finnigan LCQ mass spectrograph, sample concentration Ca 1.0 mmol dm⁻³. Magnetic susceptibility data on crushed polycrystalline samples of **1** and **2** were collected from 1.8 to 300 K using a SQUID MPMS-XL7 magnetometer.

2.2. Syntheses of (1) and (2)

An acetone solution (20 cm³) of I₂ (160 mg, 0.62 mmol) was slowly added to an acetone solution (50 cm³) of [BrClBzPy]₂[Ni(mnt)₂] (906 mg, 1 mmol) and the mixture was stirred for 2 h. MeOH (90 cm³) was then added and the mixture was allowed to stand overnight; 536 mg of black micro-crystals formed, were filtered off, washed with MeOH and dried in vacuum (yield: 86%). Anal. Calcd for C₂₀H₁₀BrClN₅NiS₄: C, 38.61; H, 1.62; N, 11.26. Found: C, 38.54; H, 1.69; N, 11.09%. IR spectrum (cm⁻¹): ν(CN), 2203 s; ν(C=C) of mnt²⁻, 1485 s. ESI-MS (*m/z*): 282.5, [BrClBzPy-H]⁺; 338.2, [Ni(mnt)₂ + H]⁻.

The procedure for preparing [IClBzPy][Ni(mnt)₂] (**2**) is similar to that for **1**. Yield 82%. Anal. Calcd for C₂₀H₁₀ClIN₅NiS₄: C, 35.87; H, 1.50; N, 10.46. Found: C, 35.81; H, 1.61; N, 10.38%. IR spectrum (cm⁻¹): ν(CN), 2205 s; ν(C=C) of mnt²⁻, 1489 s. ESI-MS (*m/z*): 329.6, [IClBzPy-H]⁺; 338.1, [Ni(mnt)₂ + H]⁻.

Black single crystals suitable for the X-ray structure analysis were obtained by evaporating the MeCN and *i*-PrOH (*v*:*v* = 1:1) mixed solution of **1** and **2** about 2 weeks at room temperature.

2.3. Determination of crystal structure

Measurements of **1** and **2** were performed on a Smart APEX CCD area detector using graphite-monochromated Mo-Kα radiation (λ = 0.71073 Å) by ω scan mode.

Table 1. Crystallographic data of **1** and **2**.

Compound	1	2
Empirical formula	C ₂₀ H ₁₀ BrClN ₅ NiS ₄	C ₂₀ H ₁₀ IClN ₅ NiS ₄
Formula weight	622.64	669.63
Description	Black block	Black block
Crystal size (mm ³)	0.35 × 0.25 × 0.15	0.40 × 0.20 × 0.10
Temperature (K)	293(2)	293(2)
Wavelength (Å)	0.71073	0.71073
Space system	Triclinic	Monoclinic
Space group	<i>P</i> $\bar{1}$	<i>C</i> 2/ <i>m</i>
Unit cell dimensions (Å, °)		
<i>a</i>	7.085(2)	17.509(5)
<i>b</i>	12.846(4)	10.245(3)
<i>c</i>	14.799(5)	13.766(4)
α	65.02(1)	90
β	80.54(1)	103.33(1)
γ	76.61(1)	90
<i>V</i> (Å ³)	1184.3(6)	2402.8(3)
<i>Z</i>	2	4
<i>D</i> _{Calcd} (g cm ⁻³)	1.746	1.851
Absorption coefficient (mm ⁻¹)	2.991	2.571
<i>F</i> (000)	618	1308
Maximum and minimum transmission	0.64 and 0.41	0.77 and 0.55
θ range (°)	2.8–25.0	2.3 < θ < 25.0
Reflection collected	5865	5937
Independent reflection (<i>R</i> _{int})	4086(0.026)	2221(0.058)
Data, restraints, parameters	4086, 0, 289	2221, 0, 163
Goodness-of-fit on <i>F</i> ²	1.037	1.004
<i>R</i> ₁ , <i>wR</i> ₂ (<i>I</i> > 2 σ (<i>I</i>))	0.0555, 0.1155	0.0506, 0.1389
<i>R</i> ₁ , <i>wR</i> ₂ (all data)	0.0779, 0.1195	0.0580, 0.1453
Largest difference peak and hole (e Å ⁻³)	0.60 and -0.91	0.89 and -0.84

The structures were solved by direct methods and refined on *F*² by full-matrix least-squares, employing Bruker's SHELXTL [27]. All nonhydrogen atoms were refined with anisotropic thermal parameters. All H atoms were placed in calculated positions, assigned fixed isotropic displacement parameters 1.2 times the equivalent isotropic *U* value of the attached atom, and allowed to ride on their respective parent atoms. Crystallographic data of **1** and **2** are listed in table 1.

3. Results and discussion

3.1. Crystal structure

ORTEP drawing of **1** with atomic labeling scheme is shown in figure 1(a). An asymmetric unit of **1** contains a Ni(mnt)₂⁻ anion and a [BrClBzPy]⁺, and the Ni(III) ion is coordinated by four sulfurs of two mnt²⁻ ligands and exhibits the expected square-planar geometry. The CN groups of Ni(mnt)₂⁻ are slightly tipped out of plane, and the deviations from the plane are 0.045 Å for N(1), 0.045 Å for N(2), -0.249 Å for N(3), and 0.368 Å for N(4). As shown in table 2, the main bond distances and angles compare well with those found in other molecular solids based on Ni(mnt)₂⁻ [15–17]. The bond lengths and angles of [BrClBzPy]⁺ are comparable to those

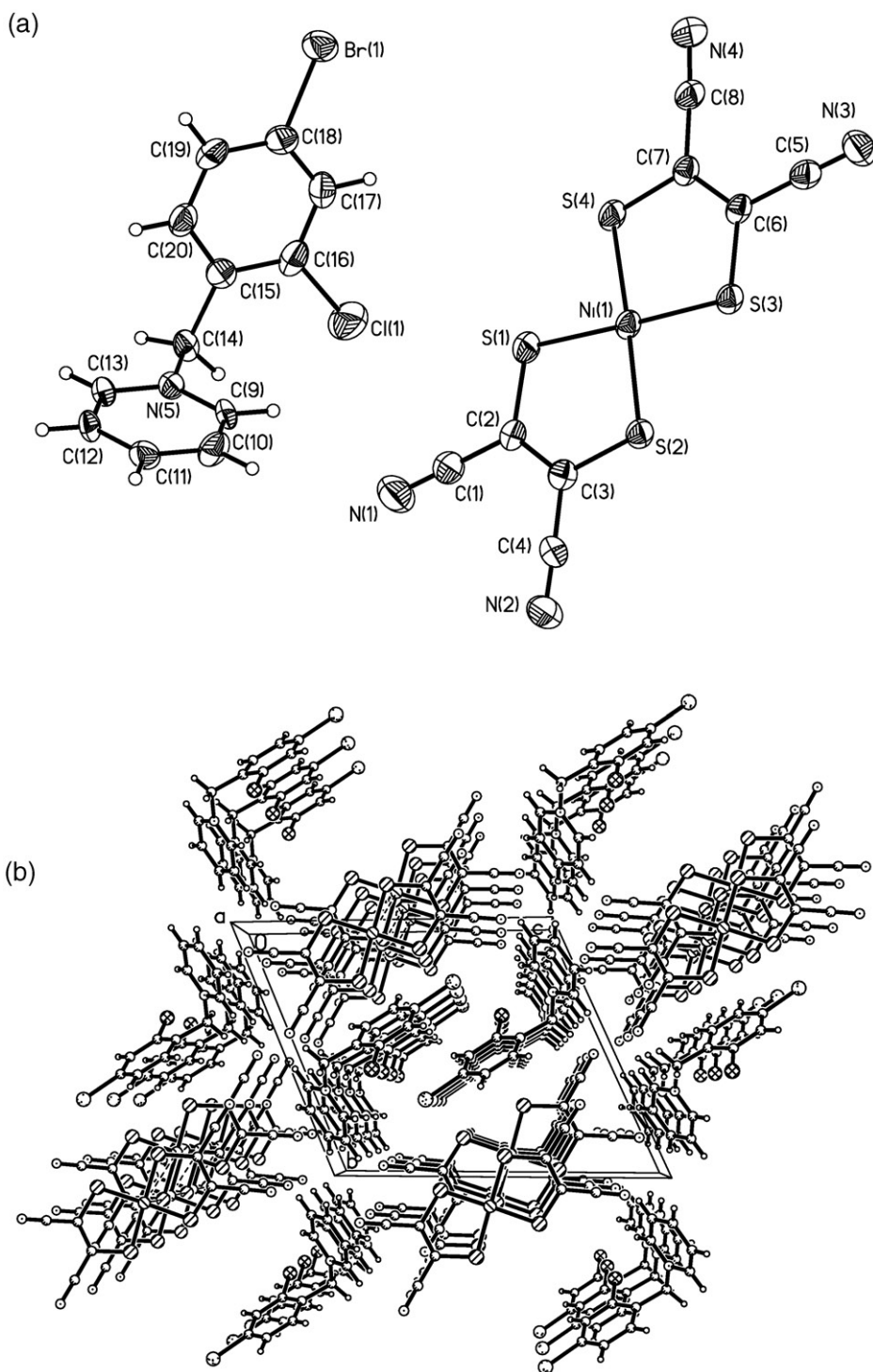


Figure 1. (a) ORTEP plot (30% probability ellipsoids) showing the molecule structure of **1**. (b) The packing diagram of a unit cell for **1** as viewed along the *a*-axis.

Table 2. Selected bond lengths and angles for **1**.

Ni(1)–S(1)	2.142(2)	C(1)–C(2)	C(1)–C(2)	1.423(9)
Ni(1)–S(2)	2.141(2)	C(2)–C(3)	C(2)–C(3)	1.380(9)
Ni(1)–S(3)	2.153(2)	C(3)–C(4)	C(3)–C(4)	1.456(8)
Ni(1)–S(4)	2.142(2)	C(5)–C(6)	C(5)–C(6)	1.436(9)
N(1)–C(1)	1.158(10)	C(6)–C(7)	C(6)–C(7)	1.377(9)
N(2)–C(4)	1.146(8)	C(7)–C(8)	C(7)–C(8)	1.415(9)
N(3)–C(5)	1.143(9)	C(9)–C(10)	C(9)–C(10)	1.364(9)
N(4)–C(8)	1.157(10)	Cl(1)–C(16)	Cl(1)–C(16)	1.709(7)
S(1)–C(2)	1.671(6)	Br(1)–C(18)	Br(1)–C(18)	1.895(7)
S(2)–C(3)	1.715(6)	N(5)–C(9)	N(5)–C(9)	1.322(8)
S(3)–C(6)	1.701(6)	N(5)–C(13)	N(5)–C(13)	1.317(8)
S(4)–C(7)	1.704(6)	N(5)–C(14)	N(5)–C(14)	1.510(8)
S(1)–Ni(1)–S(2)	92.37(7)	N(5)–C(9)–C(10)	N(5)–C(9)–C(10)	119.4(6)
S(1)–Ni(1)–S(4)	86.20(7)	N(5)–C(13)–C(12)	N(5)–C(13)–C(12)	119.1(6)
S(2)–Ni(1)–S(3)	88.88(6)	N(5)–C(14)–C(15)	N(5)–C(14)–C(15)	108.7(4)
S(3)–Ni(1)–S(4)	92.53(6)	Cl(1)–C(16)–C(15)	Cl(1)–C(16)–C(15)	122.4(5)
Ni(1)–S(1)–C(2)	103.9(2)	Cl(1)–C(16)–C(17)	Cl(1)–C(16)–C(17)	118.3(5)
Ni(1)–S(2)–C(3)	103.1(2)	Br(1)–C(18)–C(17)	Br(1)–C(18)–C(17)	119.8(5)
Ni(1)–S(3)–C(6)	102.6(2)	Br(1)–C(18)–C(19)	Br(1)–C(18)–C(19)	118.3(5)
Ni(1)–S(4)–C(7)	103.9(2)	C(9)–N(5)–C(13)	C(9)–N(5)–C(13)	122.6(6)

of [BrFBzPy][Ni(mnt)₂] [15]. The deviations of Cl and Br atoms from the phenyl ring plane are 0.077 Å for Cl(1) and –0.063 Å for Br(1). The dihedral angles between the pyridine and phenyl rings to the reference plane, C(15)–C(14)–N(5), are 107.4°(θ_1) and 66.5°(θ_2), respectively. The phenyl ring and the pyridine ring make a dihedral angle of 79.2°(θ_3). As shown in figure 1(b), well-segregated columns of anions and cations are stacked along the *a*-axis. In an anionic column, the Ni(III) ions form an alternating magnetic chain through Ni...S, S...S, or π ... π stacking interactions [figure 2(a)]. The adjacent Ni(mnt)₂[–] anions overlap in one of two patterns [figure 2(b)]: (1) pattern A with Ni(1)...Ni(1A) and Ni(1)...S(2A) distances being 4.048 Å and 3.453 Å, or (2) pattern B with Ni(1)...Ni(1B) and Ni(1)...S(2B) distances being 4.318 Å and 3.651 Å. Weak π ... π interaction occurs between Br of one phenyl ring and another phenyl ring of adjacent cations, and the contact distance of Br(1) to the neighboring benzene ring is 3.652 Å [figure 2(c)].

The coordination geometry of anion and the conformation of cation in **2**, which crystallizes in monoclinic system with space group *C2/m*, are essentially identical to those described above for **1**; bond parameters are presented in table 3. In [ClBzPy]⁺, the dihedral angles θ_1 , θ_2 , and θ_3 are 89.8°, 0°, and 89.8°, respectively. Unlike **1**, the anions and cations in **2** do not show a segregated column-like stack and adjacent anions form a tetramer [figure 3(a)]. Weak S...S and π ... π stacking interactions exist between two anions containing Ni(1) and Ni(1A) in which the shortest S...S distance is 3.614 Å, and the distance of Ni(1) to the corresponding plane is 3.593 Å. The short C...N interaction is between two anions containing Ni(1) and Ni(1B), and the C(1)...N(1) distance is 3.654 Å. It is worth noting that interactions between anions and cations were observed in the crystal structure as shown in figure 3(b): (1) π – π stacking interaction between the plane of Ni(mnt)₂[–] anion and the neighboring pyridine ring of [ClBzPy]⁺ cation with the distance between Ni(1) and the center of pyridine ring being 3.577 Å; (2) Ni(1)...N(3) interaction with the Ni(1)...N(3) distance of 3.600 Å. As listed in table 4, two weak C–H...N hydrogen bonds are found between the anion

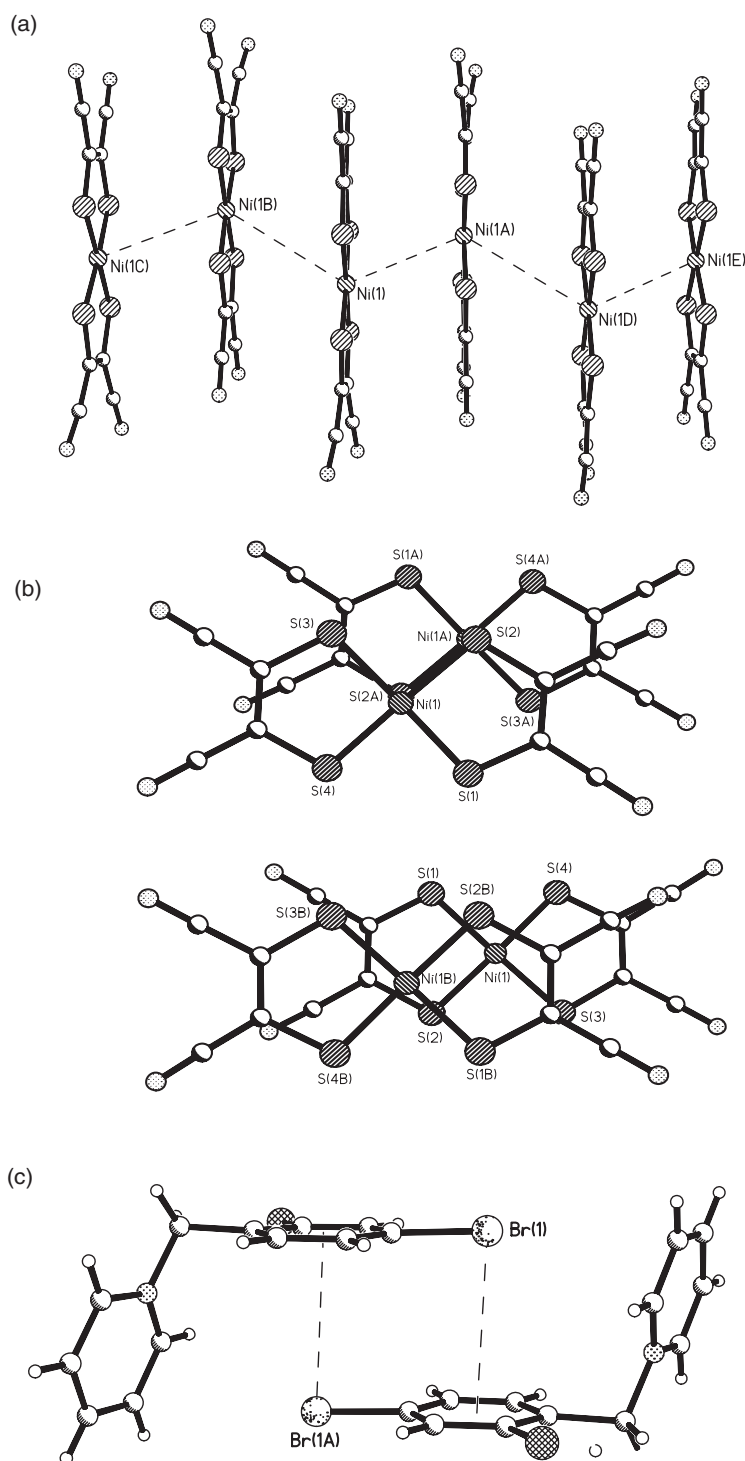


Figure 2. (a) Side view of the anion stacking of **1** showing the alternating chain. (b) The overlap of $[\text{Ni}(\text{mnt})_2]^-$ for **1**. (c) The $p \dots \pi$ interaction between the cations in **1**.

Table 3. Selected bond lengths and angles for **2**.

Ni(1)–S(1)	2.143(2)	S(1)–C(2)	1.721(4)
Ni(1)–S(2)	2.143(1)	S(2)–C(3)	1.714(4)
N(1)–C(1)	1.132(8)	Cl(1)–C(5)	1.744(6)
N(2)–C(4)	1.140(7)	I(1)–C(7)	2.081(7)
S(1)–Ni(1)–S(2)	87.27(5)	N(3)–C(11)–C(10)	113.7(5)
S(1)–Ni(1)–S(1)#1	92.60(5)	N(3)–C(12)–C(13)	119.4(5)
S(2)–Ni(1)–S(2)#1	92.83(5)	Cl(1)–C(5)–C(6)	118.6(5)
Ni(1)–S(1)–C(2)	103.12(15)	Cl(1)–C(5)–C(10)	123.1(6)
Ni(1)–S(2)–C(3)	103.30(17)	I(1)–C(7)–C(6)	119.0(5)
C(11)–N(3)–C(12)	118.7(3)	I(1)–C(7)–C(8)	120.2(7)

Note: Symmetry transformations used to generate equivalent atoms:
 #1 = $x, -y, z$.

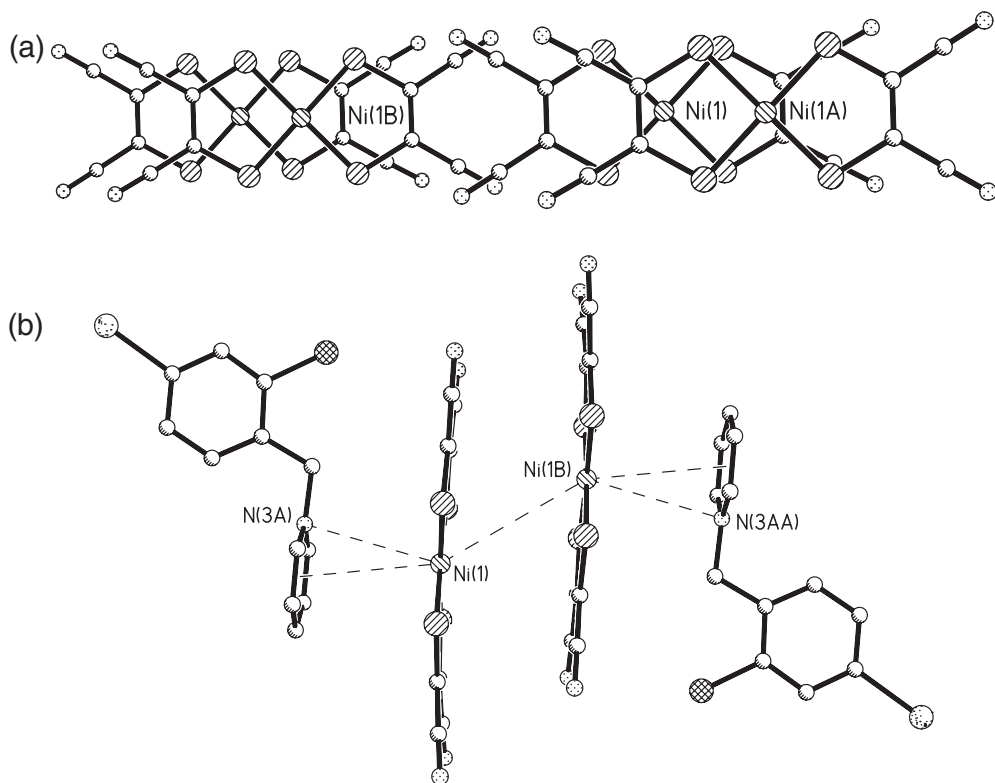


Figure 3. (a) The overlap of the anions for **2** showing a tetramer. (b) The interaction between the anions and the cations for **2**.

and the cation. These anion–anion and anion–cation interactions play important roles in the packing and stabilization of **2**.

Previous studies have indicated that the magnetic coupling between $\text{Ni}(\text{mnt})_2^-$ anions is very sensitive to the overlap of neighboring $\text{Ni}(\text{mnt})_2^-$ anions and intermolecular

Table 4. Weak hydrogen bonds for **2** (Å and °).

D–H...A	d(D–H)	d(H...A)	d(D...A)	∠(DHA)
C(11)–H(11A)...N(2)#2	0.97	2.42	3.270(5)	145.0
C(11)–H(11B)...N(2)#3	0.97	2.42	3.270(5)	145.0

Note: Symmetry transformations used to generate equivalent atoms:
 #2: $-x+1, -y+1, -z+1$; #3: $-x+1, y, -z+1$.

contacts; small structural variations can lead to large changes in the properties of molecular solids based on Ni(mnt)₂⁻ [9, 15, 16, 20]. The stacking of [M(mnt)₂]⁻ depends strongly upon the molecular topology of the countercation. Derivatives of benzylpyridinium (abbreviated as [RBzPy]⁺) serve as flexible cations which can be adjusted by modifying the groups on the aromatic rings, and the molecular configuration was determined by three dihedral angles (θ_1, θ_2 , and θ_3) [28]. When we fix Cl as the *o*-substituent and change the *p*-substituted group from Br to I atom, θ_1, θ_2 , and θ_3 changed from 107.4°(θ_1), 66.5°(θ_2), and 79.2°(θ_3) for **1** to 89.8°(θ_1), 0°(θ_2), and 89.8°(θ_3) for **2**. In **1**, the weak *p*... π interaction between Br of one phenyl ring and another phenyl ring of adjacent cations resulted in well-segregated columns of anions and cations stacked along the *a*-axis. But in **2**, there was no *p*... π interaction between I of one phenyl and the phenyl ring of an adjacent cation because of steric hindrance. By comparing the structures of **1** and **2**, we conclude that the stacking and overlap of [Ni(mnt)₂]⁻ are different when we have Cl as the *o*-substituted group and changed the *p*-substituted group with *p*-substituted Br favoring a 1-D alternating chain of Ni(mnt)₂ anions.

3.2. Magnetic properties and analyses

Variable-temperature magnetic susceptibility of **1** and **2** are shown in figure 4 in the form of $\chi_m T$ versus T . In the whole temperature range, **1** and **2** show similar magnetic behavior. At 300 K, the $\chi_m T$ values of **1** and **2** are 0.197 and 0.190 emu K mol⁻¹, respectively, less than the calculated spin-only value of 0.375 emu K mol⁻¹ for a system comprised of noninteracting $g=2, S=1/2$ spin sites indicating that significant antiferromagnetic coupling is involved. When the system cools, the values of $\chi_m T$ decrease quickly to 0.0074 emu K mol⁻¹ at 110 K for **1**, and 0.0077 emu K mol⁻¹ at 100 K for **2**, then slowly drop to zero at 1.8 K.

For **1**, the Ni...Ni distance (4.048 Å) between anions containing Ni(1) and Ni(1A) is smaller than that (4.318 Å) of the anion containing Ni(1) and Ni(1B) in the 1-D nickel(III) chains. The magnetic interaction between Ni(1) and Ni(1B) can be neglected. For **2**, the magnetic interaction between Ni(1) and Ni(1A) is larger than that between the Ni(1) and Ni(1B) ions. Thus, the magnetic susceptibility data of **1** and **2** can be fitted using a simple dinuclear model approximation (the Hamiltonian being $H = -2JS_A S_B$) [equation(1)] [29]:

$$\chi_m = \frac{(2N\beta^2 g^2 / kT)(1 - \rho)}{(3 + \exp(-2J/kT))} + (N\beta^2 g^2 / 2kT)\rho \quad (1)$$

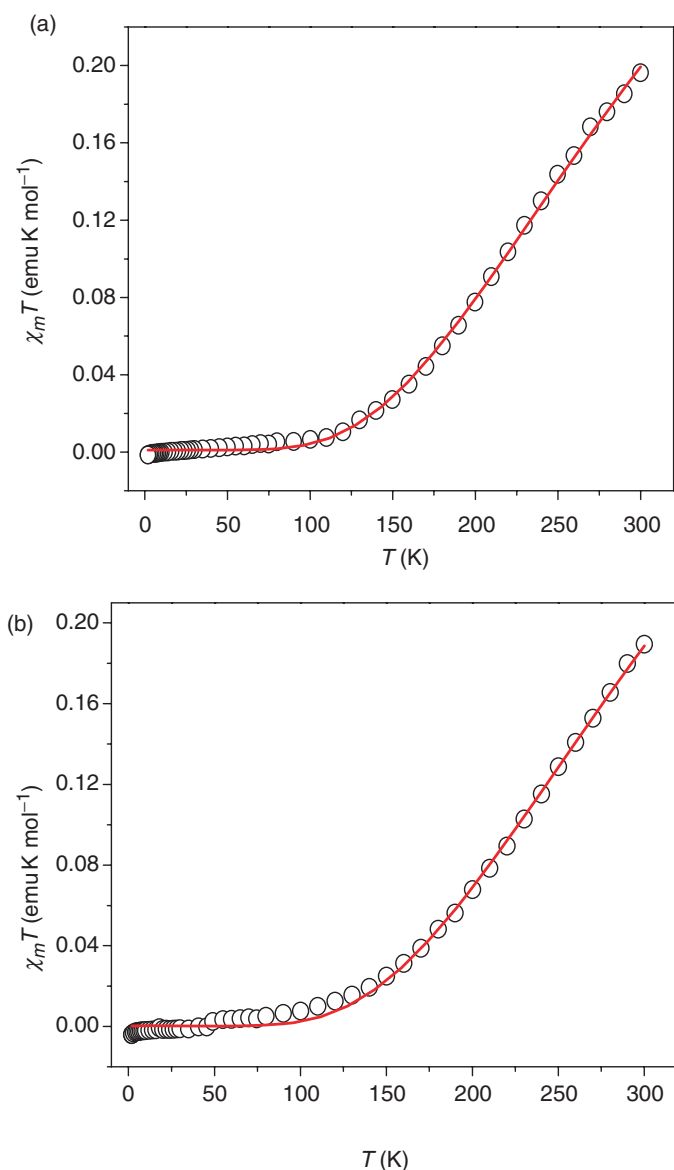


Figure 4. Plots of $\chi_m T$ vs. T for **1**(a) and **2**(b). The solid lines are reproduced from the theoretic calculations and detailed fitting procedure described in the text.

where N , g , k , β , and ρ have their usual meanings and J is the exchange coupling parameter describing the magnetic interaction between any two neighboring $S=1/2$ spins. The best-fit parameters obtained by least-squares are: $g=1.98$, $J=-231.5$ cm⁻¹, $\rho=1.8 \times 10^{-3}$, and $R=3.7 \times 10^{-6}$ for **1**, $g=1.96$, $J=-245.3$ cm⁻¹, $\rho=3.5 \times 10^{-4}$, and $R=7.9 \times 10^{-6}$ for **2** (R is defined as $\Sigma(\chi_m T^{\text{Calcd}} - \chi_m T^{\text{bsd}})^2 / \Sigma(\chi_m T^{\text{bsd}})^2$). The low ρ -values suggest that paramagnetic impurities have little effect on magnetism for **1** and **2**. The model provides an excellent fit [the solid lines in figure 4(a) represent **1** and in figure 4(b) represent **2**], as indicated by the low value of R .

4. Conclusion

Two solids, [BrClBzPy][Ni(mnt)₂] and [ClBzPy][Ni(mnt)₂], exhibiting antiferromagnetic behavior have been synthesized and their single crystal structural analyses show Ni(III) ions form a 1-D zigzag alternating chain within a Ni(mnt)₂⁻ column through Ni...S, S...S, or π ... π stacking interactions in **1**, and a tetramer in **2**. The variable temperature magnetic susceptibilities of **1** and **2** in the temperature range 1.8–300 K have been interpreted in terms of a simple dinuclear model with strong antiferromagnetic interactions.

Supplementary materials

Supplementary crystallographic data are available from the Cambridge Crystallographic Data Center, CCDC No. 298943 and No. 298947. Copies of this information may be obtained free of charge from The Director, CCDC, 12 Union Road, Cambridge, CB2 1EZ, UK (Fax: +44-1223-336033; Email: deposit@ccdc.cam.ac.uk or www: http://www.ccdc.cam.ac.uk).

Acknowledgments

The authors thank financial support from the Science and Technology Project (No. 2008B080703005) from Guangdong Science and Technology Department and the President's Science Foundation of South China Agricultural University (No. 2008 X 015).

References

- [1] C.W. Liu, R.J. Staples, J.P. Fackler. *Coord. Chem. Rev.*, **174**, 147 (1998).
- [2] H. Tanaka, O. Yoshinori, K. Hayao, S. Wakako, K. Akiko. *Science*, **291**, 285 (2001).
- [3] N. Robertson, L. Cronin. *Coord. Chem. Rev.*, **227**, 93 (2002).
- [4] T. Akutagawa, T. Nakamura. *Coord. Chem. Rev.*, **226**, 3 (2002).
- [5] E. Canadell. *Coord. Chem. Rev.*, **186**, 629 (2002).
- [6] C. Rovira. *Chem. Eur. J.*, **6**, 1723 (2002).
- [7] K. Mukai, T. Hatanaka, N. Senba, T. Nakayashiki, Y. Misaki, K. Tanaka, K. Ueda, T. Sugimoto, N. Azuma. *Inorg. Chem.*, **41**, 5066 (2002).
- [8] R. Kato, Y. Kashimura, H. Sawa, Y. Okano. *Chem. Lett.*, 921 (1997).
- [9] A.T. Coomber, D. Beljonne, R.H. Friend, J.L. Brédas, A. Charlton, N. Robertson, A.E. Underhill, M. Kurmoo, P. Day. *Nature*, **380**, 144 (1996).
- [10] S. Nishihara, T. Akutagawa, T. Hasegawa, S. Fujiyama, T. Nakamura. *J. Solid State Chem.*, **168**, 661 (2002).
- [11] H. Tanaka, K. Mao, A. Minoru, K. Tadashi, M. Takehiko. *Inorg. Chem.*, **43**, 6075 (2004).
- [12] M. Urichi, K. Yakushi, Y. Yamashita, J. Qin. *J. Mater. Chem.*, **8**, 141 (1998).
- [13] A.E. Pullen, C. Faulmann, K.I. Pokhodnya, P. Cassoux, M. Tokumoto. *Inorg. Chem.*, **37**, 6714 (1998).
- [14] J. Nishijo, E. Ogura, J. Yamaura, A. Miyazaki, T. Enoki, T. Takano, Y. Kuwatani, M. Iyoda. *Synth. Met.*, **133–134**, 539 (2003).
- [15] J.L. Xie, X.M. Ren, Y. Song, Y. Zou, Q.J. Meng. *J. Chem. Soc., Dalton Trans.*, 2868 (2002).

- [16] X.M. Ren, Q.J. Meng, Y. Song, C.L. Lu, C.J. Hu, X.Y. Chen, Z.L. Xue. *Inorg. Chem.*, **41**, 5931 (2002).
- [17] C.L. Ni, D.B. Dang, Y. Song, S. Gao, Y.Z. Li, Z.P. Ni, Z.F. Tian, L.L. Wen, Q.J. Meng. *Chem. Phys. Lett.*, **396**, 353 (2004).
- [18] D.B. Dang, C.L. Ni, Y. Bai, Z.F. Tian, Z.P. Ni, L.L. Wen, Q.J. Meng, S. Gao. *Chem. Lett.*, **5**, 680 (2005).
- [19] J.L. Xie, X.M. Ren, Y. Song, W.W. Zhang, W.L. Liu, C. He, Q.J. Meng. *Chem. Commun.*, 2346 (2002).
- [20] Z.P. Ni, X.M. Ren, J. Ma, J.L. Xie, C.L. Ni, Z.D. Chen, Q.J. Meng. *J. Am. Chem. Soc.*, **127**, 14330 (2005).
- [21] X.M. Ren, Q.J. Meng, Y. Song, C.S. Lu, C.J. Hu. *Inorg. Chem.*, **41**, 5686 (2002).
- [22] X.M. Ren, S. Nishihara, T. Akutagawa, S. Noro, T. Nakamura, W. Fujita, K. Awaga, Z.P. Ni, J.L. Xie, Q.J. Meng, R.K. Kremer. *J. Chem. Soc., Dalton Trans.*, 1988 (2006).
- [23] C.L. Ni, J.R. Zhou, Z.F. Tian, Z.P. Ni, Y.Z. Li, Q.J. Meng. *Inorg. Chem. Commun.*, **10**, 880 (2007).
- [24] X.M. Ren, T. Akutagawa, S. Nishihara, T. Nakamura, W. Fujita, K. Awaga. *J. Phys. Chem. B*, **109**, 16610 (2005).
- [25] S.B. Bulgarevich, D.V. Bren, D.Y. Movshovic, P. Finocchiaro, S. Failla. *J. Mol. Struct.*, **317**, 147 (1994).
- [26] A. Davison, R.H. Holm. *Inorg. Synth.*, **10**, 7 (1967).
- [27] SHELXTL, Version 5.10. *Structure Determination Software Programs*, Bruker Analytical X-ray Systems Inc, Madison, Wisconsin, USA (1997).
- [28] X.M. Ren, S. Nishihara, T. Akutagawa, S. Noro, T. Nakamura, W. Fujita, K. Awaga, Z.P. Ni, J.L. Xie, Q.J. Meng, R.K. Kremer. *J. Chem. Soc., Dalton Trans.*, 1988 (2006).
- [29] Y. Song, D. Zhu, K. Zhang, Y. Xu, C. Duan, X. You. *Polyhedron*, **19**, 1461 (2000).